

Stress analysis of skin wounds using advanced discretization techniques

Ana Guerra ¹, Jorge Belinha ², Renato Natal Jorge ³

¹aguerra@inegi.up.pt; INEGI, Rua Dr. Roberto Frias, 400, 4200-465; Porto; Portugal

²job@isep.ipp.pt; ISEP, Rua Dr. António Bernardino de Almeida, 431, 4249-015; Porto; Portugal

³rnatal@fe.up.pt; FEUP, Rua Dr. Roberto Frias, 4200-465 Porto, Portugal

Abstract

Human skin is the largest human organ and it is an important physical barrier that allows body homeostasis. During wound healing, this mechanically flexible organ is capable to repair itself. Nevertheless, the wound represents an abrupt change in the skin continuum, leading to stress concentrations in the surrounding wound area. Advanced discretization techniques, namely finite element method (FEM) and radial point interpolation method (RPIM), are suitable computational tools to simulate biomechanical problems allowing to analyse the displacement field and the corresponding stress and strain fields. This study aimed to construct a 2D model of skin wounds with different depths and to analyse the stress and strain fields obtained, using FEM and RPIM analysis. The simulations results demonstrated that the highest levels of stress were observed in the end of the wound, in both techniques used. Regarding the strain fields, hypodermis presented the highest values. Although this is a preliminary study to assess the performance of these numerical methods in the analysis of stress profile distribution in the human skin, it was possible to conclude that both finite element method and radial point interpolation method are valid numerical tools. Moreover, the materials used in the simulations were well characterized in terms of elasticity. In future work, it is intended to refine the model parameters and to include the hyperelastic and the anisotropic behaviour of the human skin.

Article Info

Keywords

Finite element method
Radial Point
Interpolation Method
Human skin
Stress and strain fields

Article History

Received: 02/11/2020
Revised: 30/01/2021
Accepted: 25/03/2021

DOI: 10.5281/zenodo.4837321

1 Introduction

Skin wounds can be the consequence of damage in traumatic accidents, the result of surgical incisions or of long periods of immobility or they can be associated with other pathologies, such as obesity and diabetes. Given its high frequency during human life, the treatment of skin wounds presents high economic and social costs in our society [1, 2].

Human skin is an important physical barrier between the body and the external environment. This tissue is composed by two layers: epidermis and dermis. The epidermis, the upper layer, is very thin being minimal its contribution to the mechanical behaviour of the skin. The dermis, the layer below the epidermis, has approximately 2 mm of thickness and provides the structural and the nutritional support for the skin. The dense collagen and elastin network in the dermis is responsible for the skin's mechanical properties [3]. Although not consensual, a third layer can be considered, the hypodermis, mainly composed by fat connective tissue that connects the dermis with the skeletal components. Each skin layer presents its own composition well defined and its specific mechanical properties.

When the skin is damaged wound healing takes place in order to restore the tissue homeostasis. Wound healing is usually divided in four phases: haemostasis, inflammation, proliferation and tissue remodelling [4]. For the correct skin wound healing this orderly sequence of events have to occur. Otherwise, if any step of the healing process is changed, pathogenic responses may take place leading to fibrosis or chronic wounds. In fact, injuries in the skin normally results in changes in the skin composition and in the scar formation. Scars present different mechanical response comparatively to healthy tissue. Therefore, skin wounds represent an abrupt change in the skin continuum, leading to stress concentrations in the surrounding of the wound area.

Skin computational modelling received more attention in the last few years. Indeed, computational modelling is a useful tool in surgery planning and treatment optimization [5, 6]. Some authors used advanced discretization techniques, namely finite element method (FEM) and meshless methods to predict the geometry of surgical incisions [7] and to analyse stress distribution in the skin [8] in order to reduce scar formation. In the future, it is intended that advanced discretization techniques could assist surgeons in the decision-making process when planning individual surgeries,



allowing to establish the regions with stress and strain concentration in order to improve the skin wound healing and the scar formation.

As already mentioned, stress is one of the many biological factors that plays an important role in wound healing and in scar formation. Accordingly, analyse stress theoretically is demanded, since no invasive or non-invasive technique to measure stress directly is available. It has already been shown that minimum stress is useful for producing a better scar. However, maximum stress has adverse effects in wound healing and compressive stress should be avoided since skin cannot support negative stress. Moreover, excessive tissue tension can compromise blood supply and consequently promote tissue necrosis [9]. Therefore, analysing the stress profile distribution in the skin after wounds occurrence is very important in order to address new and more effective therapies. However, as already discussed, there are no invasive or non-invasive methodologies to measure stress *in vivo* [10]. Thus, advanced discretization techniques provide an excellent alternative to predict tissue stress.

In this work, we constructed 2D models of skin wounds with different depths and we performed a linear elasto-static analysis of the stress and strain fields obtaining in each model, using both FEM and Radial Point Interpolation Method (RPIM). Moreover, the efficiency of both numerical methods used will be addressed.

2. Numerical analysis

FEM and RPIM methods are very well implemented due to their application in several areas and their possibility to deal with complicated geometries, loads and different material properties.

In FEM the domain is discretized with a finite number of interconnected elements. FEM is a mesh-dependent method, in which every element is connected, directly or indirectly, to every other elements constructing a mesh. In the generic procedure, first it is necessary to obtain the discretized mesh and then the interpolation function should be achieved. The polynomials functions are used to interpolate the field variables over the element. Then, the Galerkin method is used to obtain the discrete equation system. To find the global equation system, the local element equations for all elements used for the discretization need to be combined. Before performed the solution, the boundary conditions should be imposed. Finally, it is possible to solve the global equation system [11].

In RPIM, the problem domain is discretized with a free nodal distribution and the field functions are approximated within an influence-domain rather than an element [12, 13]. Since there is no predefined nodal interdependency in RPIM, the nodal connectivity has to be enforced after the nodal discretization. Consequently, the ‘influence-domain’ of each node, obtained by searching enough nodes inside of a fixed area, is determined. In meshless methods, the nodal distribution does not form a mesh, since the only information previously required is the spatial location of each node that discretize the problem domain. A fine nodal distribution leads, generally, to accurate results. However, the increase in the total number of nodes also increase the computational cost. Once the nodal discretization is completed, the background integration mesh should be constructed. This is necessary to numerically integrate the weak form equations governing the physic phenomenon under study. Accordingly, the integration mesh, using the Gauss-Legendre quadrature scheme, is constructed. The following step consists in establish the discrete equation system, using the approximation or interpolations shape functions. In RPIM, the interpolation shape function combines a radial basis function with a polynomial basis function to obtain the approximation. The interpolation functions possess the Kronecker delta property, which means that the obtained function passes through all scattered points in the influence domain. Accordingly, this property simplify the imposition of the essential boundary conditions [12].

3. Solid mechanics

The solids and structures become stressed when they are subject to loads or forces. This stress results in strain, which can be interpreted as deformation or relative displacements [12]. The relationship between stress and strain and the relationship between strain and displacements are the focus of solid mechanics. In this work, only linear elastic materials are considered. It means that the relationship between stress and strain is assumed to be linear and the deformation in the solid caused by loading disappears fully with the unloading. Moreover, all the materials were considered to exhibit isotropic behaviour. For this reason, the materials can be completely defined by its Elastic Modulus (E) and Poisson’s coefficient (ν). Furthermore, the relationship between the components of stress and strain can be given by the Hooke’s Law.

The present work was developed in two-dimensions, considering the plane strain or the plane stress assumptions. In this work we aim to analyse the von Mises stress and the equivalent strain obtained in skin. Accordingly, the von Mises stress for each interest point, \mathbf{x}_I , can be calculated using Eq.(1) and the equivalent strain for each interest point, \mathbf{x}_I , can also be obtained using Eq.(2). The fully description of all the concepts and formulation in this area is presented in [12].

$$\bar{\sigma}(\mathbf{x}_I) = \sqrt{\frac{1}{2}[(\sigma(\mathbf{x}_I)_1 - \sigma(\mathbf{x}_I)_2)^2 + (\sigma(\mathbf{x}_I)_2 - \sigma(\mathbf{x}_I)_3)^2 + (\sigma(\mathbf{x}_I)_3 - \sigma(\mathbf{x}_I)_1)^2]} \quad (1)$$

$$\bar{\varepsilon}(\mathbf{x}_I) = \sqrt{\frac{2}{3}[(\varepsilon(\mathbf{x}_I)_1 - \varepsilon_m)^2 + (\varepsilon(\mathbf{x}_I)_2 - \varepsilon_m)^2 + (\varepsilon(\mathbf{x}_I)_3 - \varepsilon_m)^2]} \quad (2)$$

4. Numerical model

In this work, we developed 2D models to analyse the von Mises stress and the equivalent strain in wounds with different depths, using FEM and RPIM analysis. All the numerical simulations were performed using the software FEMAS. In Fig. 1 the geometry and boundary conditions used are presented. Concerning model A, the wound is located entirely in the dermis. In model B the wound is located in the transition from the dermis to the hypodermis. Finally, in model C the wound is located until the hypodermis. In all the three models the displacement (δ) was applied to all the elements localized in the boundary in the left side. It is equal to 10% of the wound depth in the top and zero in the bottom, and all the elements in the middle have the respective displacement value. In Table 1 the model dimensions and the material properties of each skin layer used to construct the models are presented.

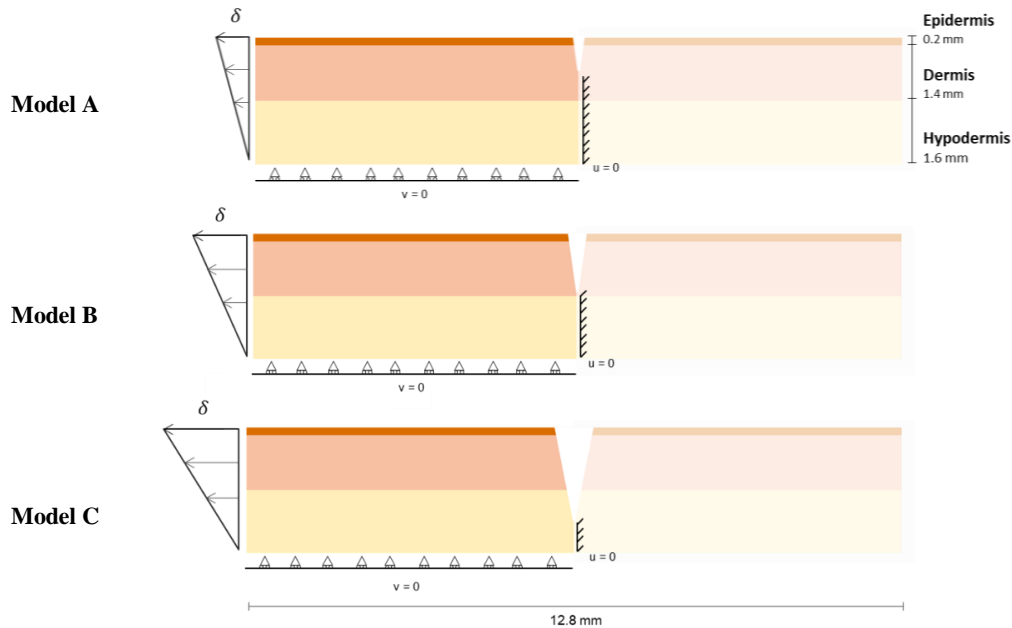


Fig. 1 - Model geometry and boundary conditions for model A, model B and model C.

Table 1 - Model dimensions and material properties.

Skin layer	Thickness - mm	Elastic Modulus (E) - MPa	Poisson's coefficient (ν)
Epidermis	0.2	102	0.48
Dermis	1.4	10.2	0.48
Hypodermis	1.6	0.0102	0.48

5. Results

The results obtained for the von Mises stress for model A, in which the wound is located entirely in the dermis, are presented in Fig. 2. Analysing the von Mises stress isomaps (Fig. 2(a)) it is possible to observe that the highest stress levels occurs in the end of the wound, in FEM and RPIM. The measurement of this parameter in specific points in the continuum of the wound (Fig. 2(b)) confirms the highest values of stress, around 1 MPa, in the end of the wound, in FEM and RPIM analysis.

The results obtained for the equivalent strain for the same model are presented in Fig. 3. Analysing the strain isomaps (Fig. 3(a)) it is possible to observe that the highest strain levels occurs in the hypodermis, in the two advanced discretization techniques used. The measurement of this parameter in specific points in the continuum of the wound (Fig.

3(b)) confirms the highest values of strain, around 0.12, in hypodermis, in FEM and RPIM. Moreover, it is possible to verify that the strain also increased in the end of the wound (around 0.04), in both FEM and RPIM methods (Fig. 3(b)).

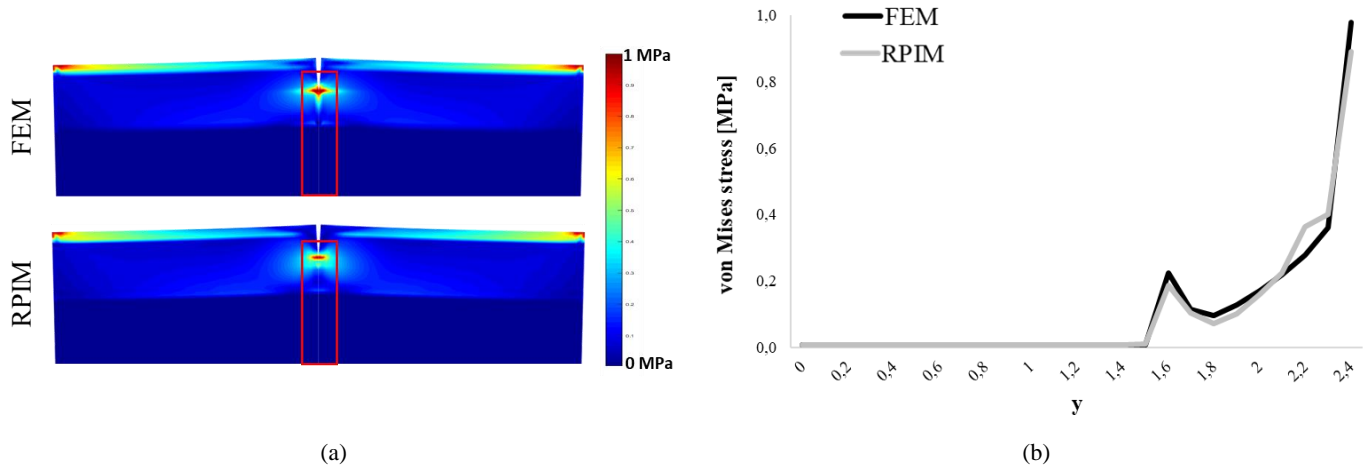


Fig. 2 - (a) von Mises stress isomaps obtained with FEM and RPIM for model A; (b) von Mises stress measured in specific points in the area marked with the rectangle in the images, in the two advanced discretization techniques.

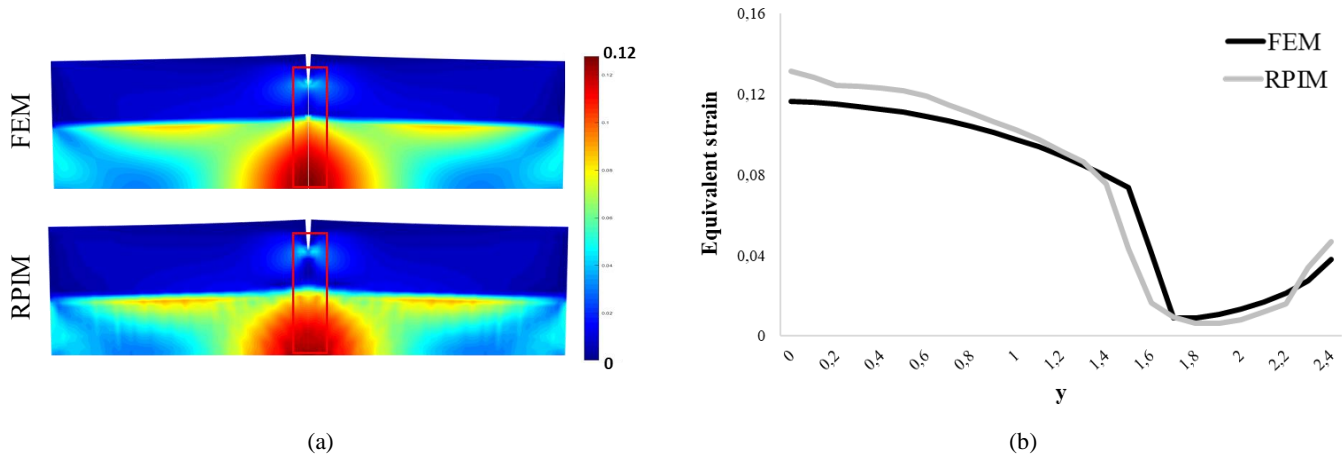


Fig. 3 - (a) Equivalent strain isomaps obtained with FEM and RPIM for model A; (b) Equivalent strain measured in specific points in the area marked with the rectangle in the images, in the two advanced discretization techniques.

The results obtained for the von Mises stress for model B, in which the wound is located in the transition from the dermis to the hypodermis, are presented in Fig. 4. Analyzing the von Mises stress isomaps (Fig. 4(a)) it is possible to observe that the stress levels in the hypodermis are very low and homogenous, in FEM and RPIM analysis. In the end of the wound, it was observed a slight increase in the stress levels, mainly in RPIM analysis. The measurement of this parameter in specific points in the continuum of the wound (Fig. 4(b)) confirms the low (around 0.01 MPa) and homogeneous levels of stress in hypodermis, in the two discretization techniques.

The results obtained for the equivalent strain for the same model are presented in Fig. 5. Analysing the equivalent strain isomaps (Fig. 5(a)) it is possible to observe that the highest strain levels occurs in the hypodermis, in FEM and RPIM analysis. The measurement of these parameters in specific points in the continuum of the wound (Fig. 5(b)) confirms the highest values of strain, around 0.25, in hypodermis, in the two discretization techniques used.

The results obtained for the von Mises stress for model C, in which the wound is located until the hypodermis, are presented in Fig. 6. Analysing the von Mises stress isomaps (Fig. 6(a)) it is possible to observe that, analogous to the previous results, the stress levels in the hypodermis were very low and homogenous, in two advanced discretization techniques. The measurement of these parameters in specific points in the continuum of the wound (Fig. 6(b)) confirms the low (around 0.01 MPa) and homogeneous levels of stress in hypodermis, in FEM and RPIM analysis. In the end of the wound, it was observed a slight increase in the stress levels, around 0.02 MPa, in the two advanced discretization techniques used.

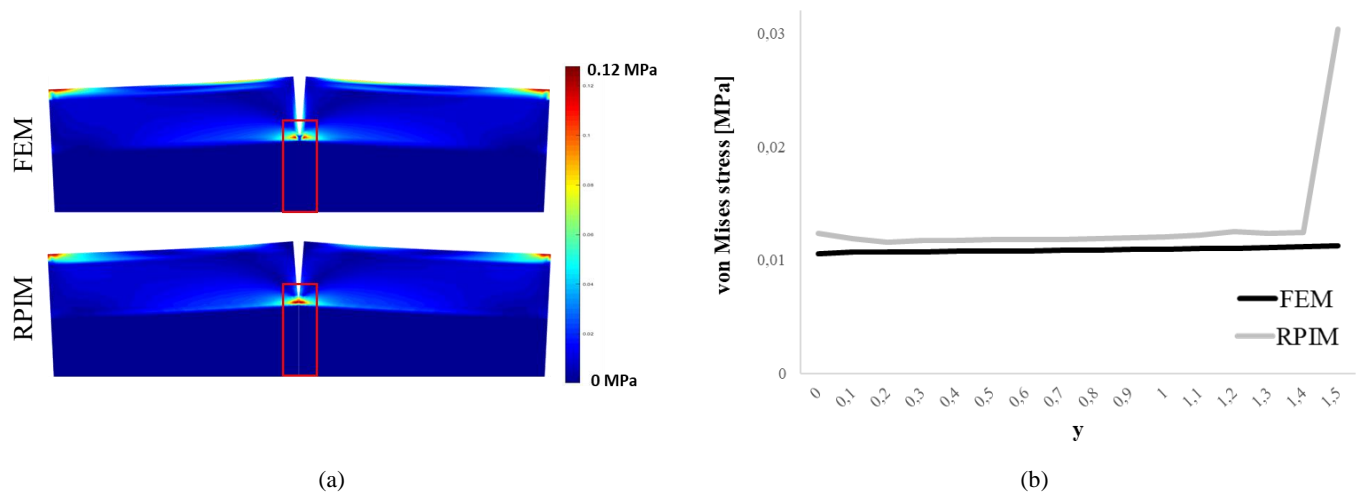


Fig. 4 - (a) von Mises stress isomaps obtained with FEM and RPIM for model B; (b) von Mises stress measured in specific points in the area marked with the rectangle in the images, in the two advanced discretization techniques.

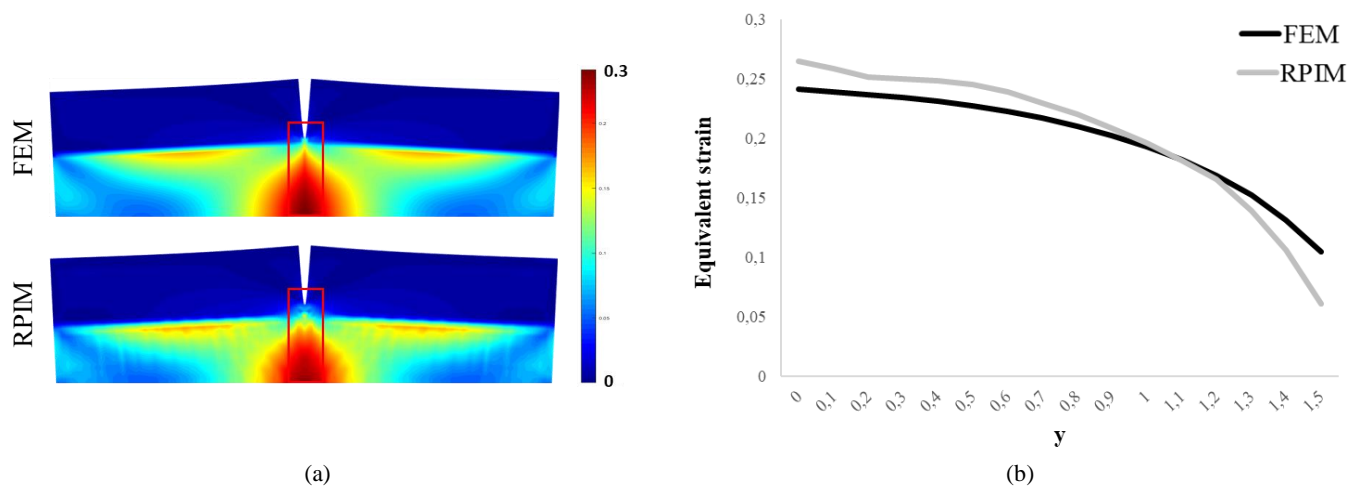


Fig. 5 - (a) Equivalent strain isomaps obtained with FEM and RPIM for model B; (b) Equivalent strain measured in specific points in the area marked with the rectangle in the images, in the two advanced discretization techniques.

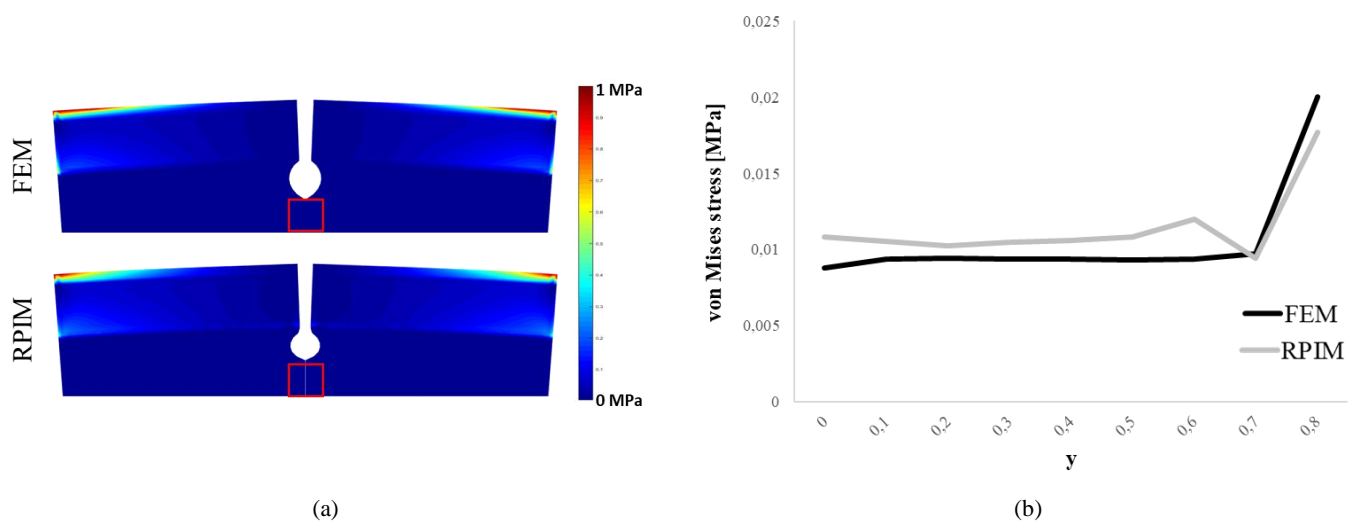


Fig. 6 - (a) von Mises stress isomaps obtained with FEM and RPIM for model C; (b) von Mises stress measured in specific points in the area marked with the rectangle in the images, in the two advanced discretization techniques.

The results obtained for the equivalent strain for the same model are presented in Fig. 7. Analysing the equivalent strain isomaps (Fig. 7(a)) it is possible to observe that the highest strain levels occurred in the area around the wound, in the two advanced discretization techniques used. The measurement of these parameters in specific points in the continuum of the wound (Fig. 7(b)) confirms the highest values of strain, around 0.5, in the area around the wound, in FEM and RPIM analysis.

6. Discussion

Computational modelling is a very useful tool to predict stress profiles around the skin wounds, especially because there no exist methodologies to measure stress *in vivo* [14]. In this work, FEM and RPIM analysis were used to study the stress and strain fields in wounds with different depths. In our model, the highest levels of stress were obtained in the end of the wound, in both used techniques. Model A presented the highest stress levels, in both FEM and RPIM analysis. In Model B and C, where the wound was located in the hypodermis, the stress fields obtained presented smaller values. Regarding the strain fields, hypodermis presented the highest values, in FEM and RPIM analysis. These observations may be due to the mechanical properties of each skin layer. Hypodermis presents a low elasticity modulus, comparatively to dermis and epidermis, being more easily deformed. Indeed, this skin layer is mainly composed by adipose tissue, being a very soft tissue. Buganza Tepole and co-workers demonstrated the potential of FEM to analyse the stress profile in skin flap designs [15]. The authors analysed the von Mises stress concentration in different flap design and concluded that the maximum stress were located at the distal and proximal edges of the flap, and the obtained von Mises stress varied between 0 and 1.50 MPa.

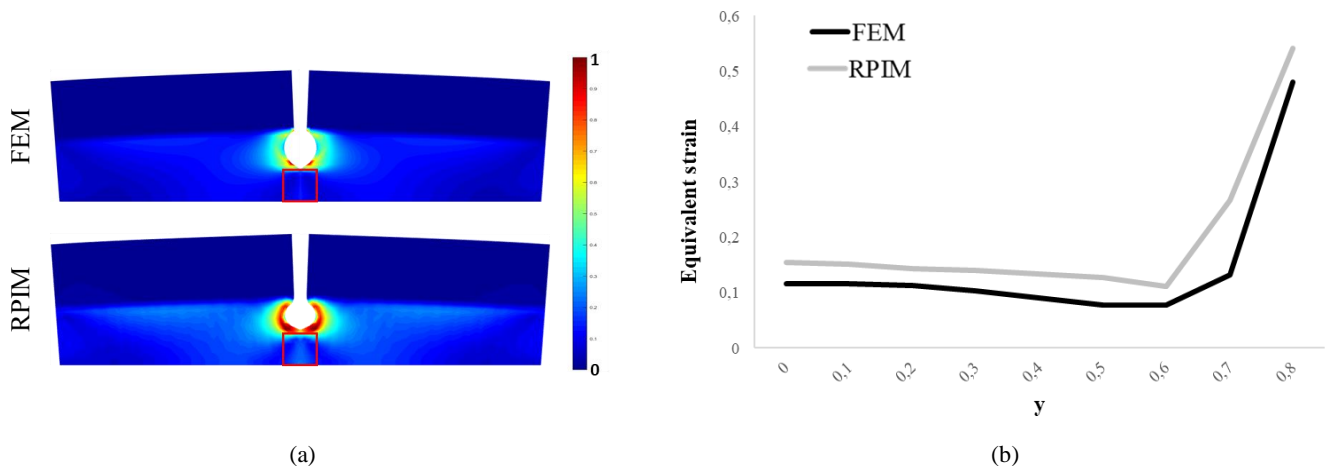


Fig. 7 - (a) Equivalent strain isomaps obtained with FEM and RPIM for model C; (b) Equivalent strain measured in specific points in the area marked with the rectangle in the images, in the two advanced discretization techniques.

Human skin exhibits nonlinear stress-strain, anisotropic and viscoelastic characteristics [16]. Nevertheless, in order to decrease the model's complexity, most of the studies assume skin as an isotropic and linear elastic material [17]. Accordingly, in this study the skin was modelled as an isotropic and linear elastic material.

Although this is a preliminary study to assess the performance of these numerical methods in the analysis of stress profile in human skin it was possible to conclude that FEM and RPIM are valid numerical tools. The numerical methods used in the simulations demonstrated equivalent results. Moreover, the materials used in the simulations were well characterized in terms of elasticity. This kind of studies can be very useful in order to achieve new approaches and methodologies to improve wound healing.

Acknowledgements and Funding

The authors truly acknowledge the funding provided by Ministério da Ciência, Tecnologia e Ensino Superior - Fundação para a Ciência e a Tecnologia (Portugal), under Grant SFRH/BD/133894/2017. Additionally, the authors acknowledge the funding provided by LAETA, under project UIDB/50022/2020.

References

- [1] Sen CK, Gordillo GM, Roy S, Kirsner R, Lambert L, Hunt TK, et al. Human skin wounds: a major and snowballing threat to public health and the economy. *Wound Repair Regen.* 2009;17(6):763-71.
- [2] Posnett J, Franks PJ. The burden of chronic wounds in the UK. *Nurs Times.* 2008;104(3):44-5.

- [3] Reihnsner R, Balogh B, Menzel EJ. Two-dimensional elastic properties of human skin in terms of an incremental model at the in vivo configuration. *Med Eng Phys.* 1995;17(4):304-13.
- [4] Singer AJ, Clark RA. Cutaneous wound healing. *N Engl J Med.* 1999;341(10):738-46.
- [5] Wang P, Becker AA, Jones IA, Glover AT, Benford SD, Greenhalgh CM, et al. Virtual reality simulation of surgery with haptic feedback based on the boundary element method. *Computers & Structures.* 2007;85(7):331-9.
- [6] Yang C, Tang D, Haber I, Geva T, del Nido PJ. In vivo MRI-based 3D FSI RV/LV models for human right ventricle and patch design for potential computer-aided surgery optimization. *Computers & Structures.* 2007;85(11):988-97.
- [7] Flynn C. Finite element models of wound closure. *J Tissue Viability.* 2010;19(4):137-49.
- [8] Lott-Crumpler DA, Chaudhry HR. Optimal patterns for suturing wounds of complex shapes to foster healing. *J Biomech.* 2001;34(1):51-8.
- [9] Toutain CE, Brouchet L, Raymond-Letron I, Vicendo P, Bergès H, Favre J, et al. Prevention of Skin Flap Necrosis by Estradiol Involves Reperfusion of a Protected Vascular Network. *Circulation Research.* 2009;104(2):245-54.
- [10] Whitcher FD. Simulation of in vivo loading conditions of nitinol vascular stent structures. *Computers & Structures.* 1997;64(5):1005-11.
- [11] Fish J, Belytschko T. *A First Course in Finite Elements*: John Wiley & Sons; 2007.
- [12] Belinha J. *Meshless Methods in Biomechanics - Bone Tissue Remodelling Analysis*: Springer International Publishing; 2014.
- [13] Belytschko T, Krongauz Y, Organ D, Fleming M, Krysl P. Meshless methods: An overview and recent developments. *Computer Methods in Applied Mechanics and Engineering.* 1996;139(1-4):3-47.
- [14] Cerda E. Mechanics of scars. *Journal of Biomechanics.* 2005;38(8):1598-603.
- [15] Tepole AB, Gosain AK, Kuhl E. Computational modeling of skin: Using stress profiles as predictor for tissue necrosis in reconstructive surgery. *Computers & structures.* 2014;143:32-9.
- [16] Silver FH, Freeman JW, DeVore D. Viscoelastic properties of human skin and processed dermis. *Skin Res Technol.* 2001;7(1):18-23.
- [17] Zahouani H, Pailler-Mattei C, Sohm B, Vargiolu R, Cenizo V, Debret R. Characterization of the mechanical properties of a dermal equivalent compared with human skin in vivo by indentation and static friction tests. *Skin Res Technol.* 2009;15(1):68-76.